





Thermodynamics of pure fast solar wind: radial evolution of the temperature–speed relationship in the inner heliosphere

Denise Perrone ¹★†, D. Stansby ¹, T. S. Horbury ¹ and L. Matteini ²

¹Department of Physics, Imperial College London, London SW7 2AZ, UK

²LESIA, Observatoire de Paris, Université PSL, CNRS, Sorbonne Université, Univ. Paris Diderot, Sorbonne Paris Cité, 5 Place Jules Janssen, 92195 Meudon, France

Accepted 2019 July 2. Received 2019 June 11; in original form 2019 April 26

ABSTRACT

A strong correlation between speed and proton temperature has been observed, across many years, on hourly averaged measurements in the solar wind. Here, we show that this relationship is also observed at a smaller scale on intervals of a few days, within a single stream. Following the radial evolution of a well-defined stream of coronal-hole plasma, we show that the temperature–speed (T – V) relationship evolves with distance, implying that the T – V relationship at 1 au cannot be used as a proxy for that near the Sun. We suggest that this behaviour could be a combination of the anticorrelation between speed and flux-tube expansion factor near the Sun and the effect of a continuous heating experienced by the plasma during the expansion. We also show that the cooling index for the radial evolution of the temperature is a function of the speed. In particular, T_{\perp} in faster wind, although higher close to the Sun, decreases more quickly with respect to slower wind, suggesting that it has less time to interact with the mechanism(s) able to heat the plasma. Finally, we predict the expected T – V relationship in fast streams closer to the Sun with respect to the *Helios* observations, which *Parker Solar Probe* will explore in the near future.

Key words: Sun: corona – Sun: heliosphere – solar wind.

1 INTRODUCTION

For decades, *in situ* observations of solar wind at 1 au have shown that the proton temperature increases with the large-scale, i.e. averaged on hours, wind speed (Neugebauer & Snyder 1966; Strong et al. 1966; Burlaga & Ogilvie 1970). This strong correlation between temperature and speed is generally used to define an expected temperature from the measured bulk velocity, giving for example a criterion to identify interplanetary mass ejections when the measured temperature is lower than half of the expected one (Richardson and Cane 1995). However, the physical origin of the temperature–speed (T – V) relationship is not clear.

Several studies of the solar wind in the ecliptic, based on hourly averaged data sets, have been focused on fitting the T – V relationship by using various functional forms (i.e. linear, quadric, and polynomial expressions). For example, Lopez & Freeman (1986) used normalized data from *Helios* 1 and found evidence for a separate law in slow and fast wind; in particular, the best fit for $V < 500 \text{ km s}^{-1}$ is a quadratic (or cubic) dependence of

temperature on velocity, while a linear dependence describes better the data for $V > 500 \text{ km s}^{-1}$. Recently, Elliott et al. (2012) performed an extensive analysis of the T – V relationship of the solar wind by means of a combination of missions at various distances, removing any transient events, to study both its temporal and radial variations. They found that, close to Earth, the T – V relationship can be globally described by a single linear fit over a speed range covering both slow and fast wind. However, the slope presents a year-to-year variation, which reflects the source properties varying with the solar cycle, along with a continued evolution with distance, due to the dynamic interactions between slow and fast wind. Moreover, the solar-wind temperature strongly depends itself on the heliocentric distance, since it does not decrease purely adiabatically during the expansion (Marsch et al. 1982; Hellinger et al. 2011, 2013).

Some theoretical mechanisms have been proposed to explain the observed temperature–speed correlation. Matthaeus, Elliott & McComas (2006) suggested that the linear dependence between T and V is a consequence of a symmetry of the solar-wind transport equations. Under the hypothesis of a spherical, constant-speed expansion, they proposed a specific heating model of magnetohydrodynamics (MHD) turbulence with a heating rate that is a function only of the convective age (i.e. the time spent by the plasma since its departure from the Sun). On the other hand, Démoulin (2009) suggested that the T – V relationship, in an open magnetic field

* E-mail: d.perrone@imperial.ac.uk, denise.perrone@asi.it

† Present address: ASI - Italian Space Agency, via del Politecnico snc, 00133 Rome, Italy.

Table 1. Intervals of unperturbed coronal-hole plasma used in this study, observed by both *Helios* probes.

Interval	Year	Start		End		Spacecraft	R (au)	V_{sw} (km s ⁻¹)	n_p (cm ⁻³)	T_p (10 ³ K)	B (nT)
		Day	UT	Day	UT						
1	1976	105	14	113	01	<i>Helios 2</i>	0.30	699.5	24.1	684.6	41.6
2	1976	74	10	79	13	<i>Helios 1</i>	0.42	611.4	15.3	383.5	23.3
3	1976	113	10	116	21	<i>Helios 1</i>	0.58	657.0	6.7	310.2	12.2
4	1976	75	04	78	03	<i>Helios 2</i>	0.65	621.2	5.0	261.6	10.9
5	1975	306	08	308	00	<i>Helios 1</i>	0.76	666.4	4.1	236.6	8.5
6	1976	48	21	51	20	<i>Helios 2</i>	0.88	640.2	2.8	198.5	7.0
7	1976	21	21	25	10	<i>Helios 2</i>	0.98	636.7	2.5	198.7	6.2

configuration plasma, is the result of the solar-wind acceleration and heating close to the Sun. In fact, since the approximation of a constant speed is reasonable only far from the Sun, both internal-energy and moment equations needed to be considered. This implies that, for a fixed distance and heating flux, the temperature is a quadratic function of the velocity (Démoulin 2009).

All previous studies on the correlation in the solar wind between proton temperature and radial velocity have been based on a large amount of data, typically using hourly averaged data and sampling many streams across multiple solar rotations, providing statistical results on how the mean plasma temperature is related to the wind speed. Recently, Perrone et al. (2019) performed a thorough analysis of the radial evolution of unperturbed coronal-hole plasma, by following single streams of solar wind, generated by specific sources, from 0.3 au to Earth. They exploited a period of solar minimum, when both the *Helios* probes observed the interplanetary plasma consisting of a series of long-lived, high-speed streams separated by slower moving plasma. The 27-d recurrence pattern offered the opportunity to study the characteristics of a plasma, originating from the same region, as they evolved with distance. A near-Sun fast stream was previously analysed by Horbury, Matteini & Stansby (2018), where small-scale enhancements in plasma speed have been identified. They also showed that the bulk fast wind has a well-established positive T – V correlation, demonstrating for the first time that such correlation is a characteristic that persists within an individual solar-wind stream. Moreover, both proton parallel and perpendicular temperatures have a clear dependence on speed.

In this paper, we focus on the radial evolution of a well-defined stream of coronal-hole plasma in the inner heliosphere, which maintains its identity during several solar rotations. By means of 40 s temperature measurements from both the *Helios* probes, we quantitatively study the T – V relationship at different radial distances. We find that the proton-core temperature is correlated with the bulk speed within each interval and this relationship evolves, within the same stream, as the plasma travels away from the Sun. Thus, the T – V relationship at 1 au cannot be used as a proxy for the relation near the Sun. Moreover, we find that the cooling index for the radial evolution of the temperature is a function of the speed, implying that the decrease of the temperature depends on the expansion time. Finally, a prediction of the temperature–speed relationship at the heliospheric distance of the first three perihelia of *Parker Solar Probe* is presented.

2 UNPERTURBED CORONAL-HOLE PLASMA

We use reprocessed particle data from the *Helios* mission (Stansby 2017; Stansby et al. 2018), where only the core of the proton distribution function is taken into account, near the minimum of

the solar activity and we consider only intervals of pure high-speed plasma that originated in coronal holes (Perrone et al. 2019). Since these coronal holes are stable over multiple solar rotations, the two *Helios* probes observed recurrent high-speed intervals at different distances from the Sun. This allows us to investigate the radial evolution of a homogeneous data set of pure fast wind, assuming that temporal variations and/or variations with heliographic latitude are absent or not important. In particular, we focus on the detected stream A in Perrone et al. (2019), which contains nine intervals of fast wind from 0.3 to 0.98 au. However, since we are interested in studying the temperature–speed relationship, we consider a 30-min running-average speed, $V = \sqrt{\langle V_r \rangle^2 + \langle V_t \rangle^2 + \langle V_n \rangle^2}$, to effectively remove speed variations due to the presence of Alfvénic spikes (Horbury et al. 2018). This means that we have to neglect intervals with several gaps in the data that could give misleading information in the estimation of the running average. This is the case for intervals A2 and A4 in Perrone et al. (2019), which now are excluded from our analysis. The unperturbed coronal-hole plasma events used in the present study and their typical parameters, averaged within each individual interval, are collected in Table 1.

2.1 Radial variation of the temperature–speed relation

A homogeneous stream of solar wind, generated by the same coronal hole and observed at different radial distances from the Sun, allows us to study how the T – V relationship evolves during the radial expansion, independently of changes of the source or stream–stream interactions. Fig. 1 shows the dependence of $T_p = (2T_{\perp} + T_{\parallel})/3$ (left-hand columns), T_{\parallel} (middle columns), and T_{\perp} (right-hand columns) on the solar-wind speed for three different radial distances, namely 0.42 au (top rows), 0.65 au (middle rows), and 0.98 au (bottom rows). The black lines indicate the least-squares linear regression function in both normal ($T \propto mV$, dashed line) and logarithmic ($T \propto V^{\gamma}$, solid line) space. The two curves almost overlap in the range where most of the points are distributed. We also provide the Pearson correlation coefficient, R_p , which gives a measure of how linear is the relationship between temperature and speed (Borovsky, Thomsen & Elphic 1998, and references therein). The 95% degree of confidence for the linear correlation is $|R_p| > R_{\text{rnd}}$, where $R_{\text{rnd}} = 2/\sqrt{N}$, N being the number of data points. The parameters for both linear and exponential fits, along with the Pearson correlation coefficients, for each interval of the present stream, are given in Table 2, where low values of R_p , due to a greater data scatter, correspond almost to flatter T – V relationships. However, the level of confidence is high in all intervals.

Unlike previous analyses that used hourly averages of plasma data and considered several streams, here we are considering a single stream of fast solar wind and analysing variation of the temperature

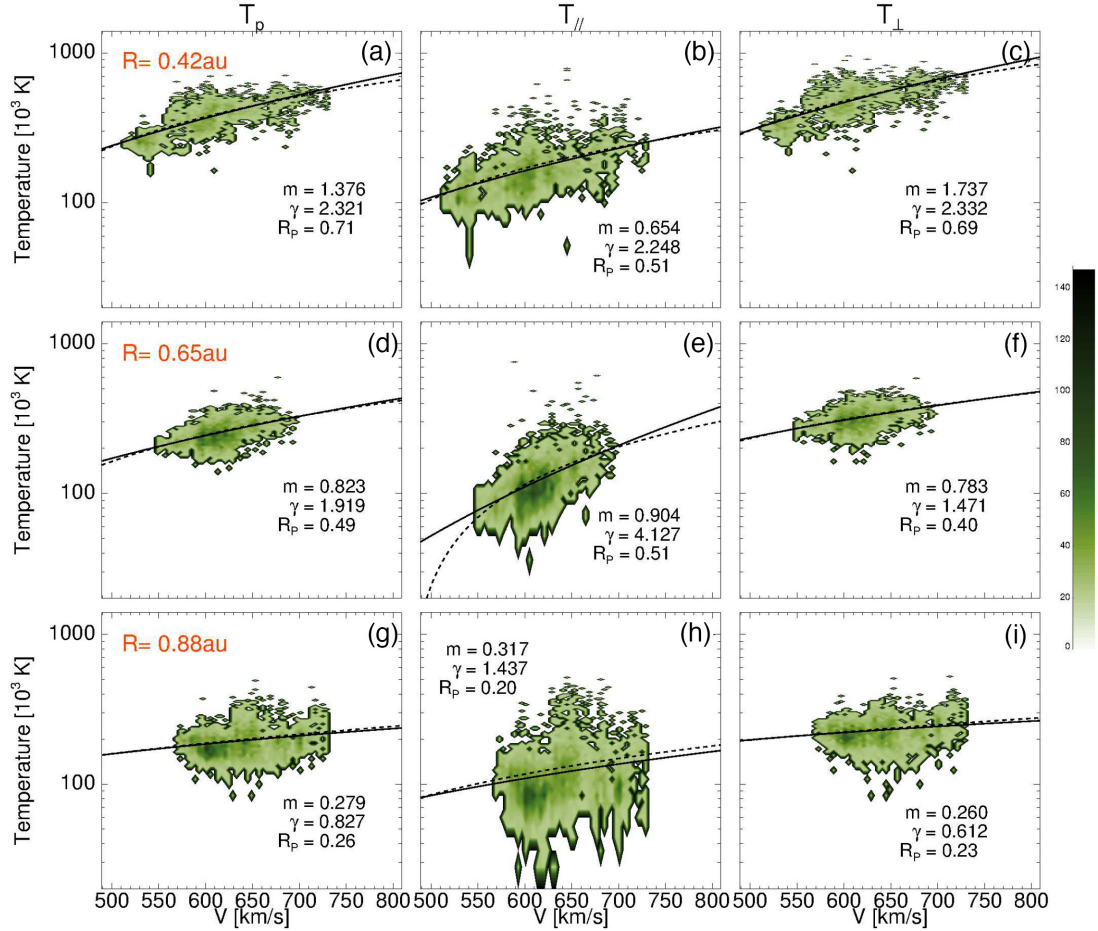


Figure 1. Radial evolution of the temperature–speed relation for T_p (left-hand column), $T_{||}$ (middle column), and T_{\perp} (right-hand column) for three different radial distances, i.e. 0.42 au (top row), 0.65 au (middle row), and 0.88 au (bottom row). Black lines refer to the fits $T \propto V^{\gamma}$ (solid) and $T \propto mV$ (dashed), where m is in unit of 10^3 K s km $^{-1}$.

at small scales (~ 40 s). The dependence of the temperature on speed is evident within each considered interval and, although a considerable scatter is observed for the parallel temperature, the linear dependence between speed and both T_{\perp} and $T_{||}$ is remarkable. Interestingly, we observe that dependence of temperature on speed evolves with distance within the same stream.

The dependence of temperature on speed could be related to the solar source of the wind, which sets the amount of energy intrinsically available to accelerate and heat the plasma. Different coronal holes can produce winds with different T – V relations, reflecting the properties of the source, set in the corona and below, even at 1 au. Elliott et al. (2012) suggested that within 0.52 au the T – V relationship should be shaped by the characteristics of the source; then, its evolution should be related to the dynamic interaction between slow and fast streams. Here, however, we interestingly observe a radial evolution of the T – V relationship within a same stream of pure coronal-hole plasma (i.e. plasma generated by the same, almost stable, source) and in the absence of stream–stream interactions. Therefore, although the initial dependence could be given by the source variability, the T – V relationship is also affected by the expansion and/or by mechanism(s) locally acting in the plasma. Moreover, since the relation for $T_{||}$ is flatter and characterized by a wider spread of the distribution with respect to T_{\perp} , the T – V relationship shows that at a given distance high speeds are linked to much higher temperature in the perpendicular

direction. Therefore, the mechanisms responsible to produce the observed correlations are able to preferentially act in the direction perpendicular to the magnetic field.

2.2 Dependence of the cooling index on speed

Local measurements of the proton temperature, within a single stream of fast solar wind, have shown a positive correlation between temperature and flow speed, which evolves as the plasma travels away from the Sun (see Fig. 1). Moreover, the proton temperature exhibits a strong dependence on the heliocentric distance (Perrone et al. 2019). Therefore, temperature is a function of both speed and radial distance, i.e. $T \equiv T(V, R)$.

By using the linear fit that describes the T – V relationship within each individual interval, i.e. at different radial distances, we extrapolate the values of the temperature for fixed values of the speed, V_0 . We choose V_0 from 550 to 800 km s $^{-1}$, in 50 km s $^{-1}$ steps, to cover all the range of typical speeds for fast wind. Fig. 2 shows, from top to bottom, the radial evolution of $T_p(V_0)$, $T_{||}(V_0)$, and $T_{\perp}(V_0)$, for three values of V_0 . Different symbols and colours refer to different values of the speed (see legend). In order to have a lighter layout, only error bars from the intermediate-speed value of 650 km s $^{-1}$, estimated from the fit of each T – V relationship, are reported in the panels. Furthermore, a least-squares linear regression function in logarithmic space has been used to fit the data (lines).

Table 2. Fit parameters, m and γ , and correlation coefficients, R_p , for the temperature–speed relationship at different radial distances. Speed is in km s^{-1} , temperatures in 10^3 K .

R (au)	m (10^3 K s km^{-1})	γ	R_p	R_p/R_{rhd}
T_p versus V				
0.30	1.15 ± 0.03	1.23 ± 0.03	0.39	20.2
0.42	1.38 ± 0.02	2.32 ± 0.03	0.71	23.3
0.58	1.02 ± 0.04	2.14 ± 0.07	0.61	11.4
0.65	0.82 ± 0.02	1.92 ± 0.05	0.49	17.1
0.76	0.55 ± 0.05	1.76 ± 0.13	0.31	5.5
0.88	0.28 ± 0.01	0.83 ± 0.04	0.26	9.7
0.98	0.48 ± 0.02	1.49 ± 0.05	0.34	13.9
T_{\parallel} versus V				
0.30	0.60 ± 0.02	1.68 ± 0.04	0.32	16.7
0.42	0.65 ± 0.02	2.25 ± 0.05	0.51	16.7
0.58	0.59 ± 0.04	2.43 ± 0.12	0.41	7.6
0.65	0.90 ± 0.02	4.13 ± 0.09	0.51	17.8
0.76	0.57 ± 0.05	3.45 ± 0.23	0.29	5.1
0.88	0.32 ± 0.02	1.44 ± 0.09	0.20	7.4
0.98	0.42 ± 0.02	1.78 ± 0.07	0.26	10.5
T_{\perp} versus V				
0.30	1.42 ± 0.04	1.17 ± 0.03	0.36	19.1
0.42	1.74 ± 0.03	2.33 ± 0.03	0.69	22.8
0.58	1.24 ± 0.04	2.06 ± 0.07	0.61	11.5
0.65	0.78 ± 0.03	1.47 ± 0.05	0.40	13.9
0.76	0.54 ± 0.06	1.41 ± 0.13	0.26	4.6
0.88	0.26 ± 0.02	0.61 ± 0.04	0.23	8.6
0.98	0.50 ± 0.02	1.42 ± 0.06	0.32	12.8

Finally, expected temperature values for $V_0 = 650 \text{ km s}^{-1}$ at $\sim 35 R_{\odot}$ (blue-filled band), where R_{\odot} is the solar radius, which corresponds to the heliospheric distance of the first three perihelia for *Parker Solar Probe*, are indicated by blue stars.

As expected, larger values of the speed are associated with higher values of the temperature. Interestingly, we observe that the cooling index, ξ , where $T \propto R^{-\xi}$ is a function of the speed (see Table 3). To better appreciate this behaviour in Fig. 3 we show $\xi(V)$ for both T_{\parallel} (violet squares) and T_{\perp} (orange circles). We find that the radial decrease of T_{\perp} becomes steeper, i.e. the cooling index increases, as the speed increases ($\xi_{\perp} \propto V_0^{(0.28 \pm 0.02)}$). A similar behaviour is observed for the total temperature, i.e. $\xi_T \propto V^{(0.15 \pm 0.01)}$ (not shown). This corresponds to a ΔT_{\perp} of about 10^5 K at 0.3 au in the slower stream, if we consider a same temperature at 1 au for two fast streams characterized by a constant speed of 550 and 800 km s^{-1} , respectively. Therefore, this behaviour suggests that, since plasma in slower streams spends more time covering the same distance with respect to faster streams, it could have more time to interact with the mechanisms able to locally increase the perpendicular (and correspondingly the total) temperature. An opposite behaviour is observed for T_{\parallel} , where the slope becomes less steep with the speed ($\xi_{\parallel} \propto V^{-(0.75 \pm 0.07)}$), even if here the errors are important due to the scatter in the distribution of the parallel temperature versus speed. Therefore, the behaviour of $\xi_{\parallel}(V)$ should be considered carefully.

2.3 Implications for new solar missions

The evolution of the T – V relationship in the inner heliosphere within a stream originating from the same source on the Sun is also relevant for new solar missions. *Parker Solar Probe* (Fox et al. 2016), launched in 2018 August, will allow a study of the dependence

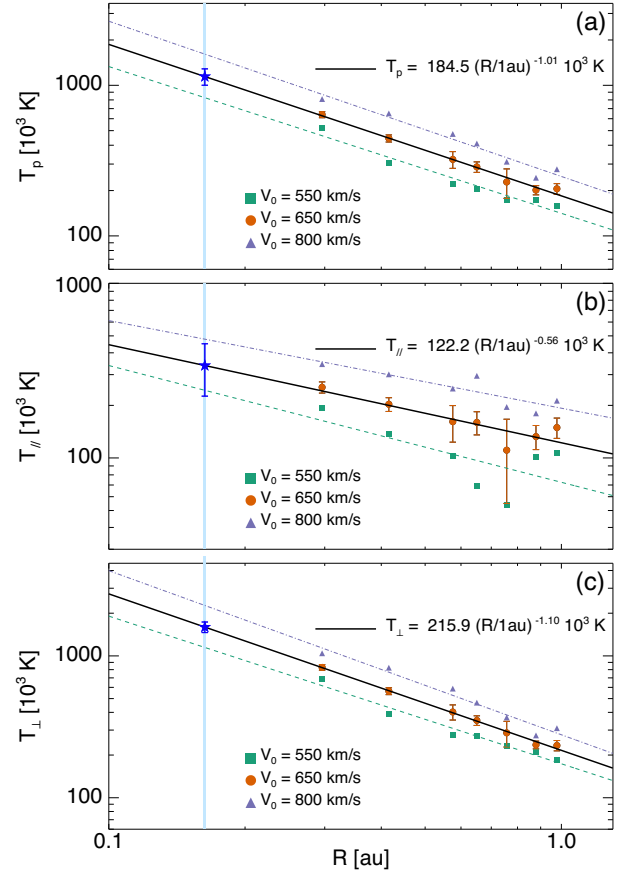


Figure 2. From top to bottom, radial evolution of $T_p(V_0)$, $T_{\parallel}(V_0)$, and $T_{\perp}(V_0)$ for three different values of V_0 (see legend). Lines show the linear fits in logarithmic space. Blue stars refer to extrapolated values of the temperature for $V_0 = 650 \text{ km s}^{-1}$ at $\sim 35 R_{\odot}$ (blue-filled band).

Table 3. Summary of the cooling index changes with the flow speed.

V_0 (km s^{-1})	ξ_T	ξ_{\parallel}	ξ_{\perp}
550	0.975 ± 0.099	0.67 ± 0.33	1.04 ± 0.08
600	0.992 ± 0.060	0.60 ± 0.20	1.08 ± 0.04
650	1.006 ± 0.050	0.56 ± 0.14	1.10 ± 0.04
700	1.016 ± 0.063	0.54 ± 0.12	1.12 ± 0.06
750	1.024 ± 0.082	0.52 ± 0.12	1.14 ± 0.08
800	1.031 ± 0.099	0.50 ± 0.13	1.16 ± 0.10

of the temperature on the speed in an environment much closer to the Sun with respect to the *Helios* orbits and, if it will encounter fast streams, could confirm the observed trend of increasing temperature gradient much closer to the source. In Fig. 4, in colour-filled contour plots, we show the expected T – V relationship in fast solar wind at $\sim 35 R_{\odot}$, corresponding to the heliospheric distance for the first three perihelia of *Parker Solar Probe* (until 2019 September). The corresponding distributions at 1 au have been also shown as contour lines, which should be compared with the fits of T_p versus V for fast wind ($V > 500 \text{ km s}^{-1}$) at solar minimum by Lopez & Freeman (1986) ($m = 0.51 \pm 0.01$ and $\gamma = 1.78 \pm 0.04$) and the more recent one by Elliott et al. (2012) covering both slow and fast speed range ($m = 0.598$). Unlike the previous analyses that use the cooling index for the temperature independent of the speed in order to remove the

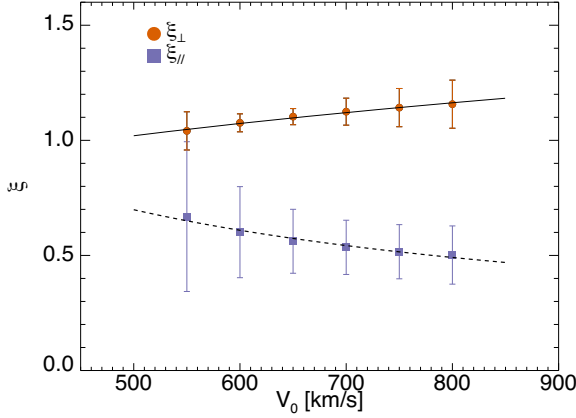


Figure 3. Cooling index as a function of the flow speed for both parallel (squares) and perpendicular (circles) temperature. Linear fits in logarithmic space are reported by lines.

effects of varying radial distance, we have extrapolated the values of the temperature within each interval listed in Table 1, by using the speed-dependent cooling indices (see Fig. 3). We observe that, closer to the Sun, the gradients of T_p and T_{\perp} become steeper, as we expected from Fig. 1 (see also Table 4). It is worth pointing out that the value of the temperature could be lower than the one predicted from *Helios* data, since the magnetic flux, which regulates the energy and particle fluxes, has decreased during the last decades (Schwadron and McComas 2008).

Thanks to *Parker Solar Probe*, by crossing the Alfvén region, it will be possible to have information about the physical mechanisms acting in the acceleration region of the solar wind and how important they are for the thermodynamics of such collisionless plasma. On the other hand, *Solar Orbiter* (Muller et al. 2013), expected launch in 2020 February, thanks to the synergy between *in situ* and remote sensing observations, will provide insight into the dependence of the temperature–speed relationship on the source, and its small-scale variations, of individual streams.

3 DISCUSSIONS

The T – V relationship is not only a global characteristic of the solar wind, but it is a typical feature of each single magnetic flux tube within a coronal hole. The flow along each flux tube, which extends from the Sun to the Earth, is characterized by a magnetic expansion factor, f_s , that is empirically anticorrelated with the asymptotic solar-

Table 4. Fit parameters and correlation coefficients for temperature–speed relation at $35 R_{\odot}$ and 1 au. Speed is in km s^{-1} , temperatures in 10^3 K .

Relation	m (10^3 K s km^{-1})	γ
$R = 35 R_{\odot}$		
T_p versus V	2.75 ± 0.03	1.65 ± 0.01
$T_{ }$ versus V	0.76 ± 0.01	1.50 ± 0.02
T_{\perp} versus V	3.90 ± 0.03	1.70 ± 0.01
$R = 1 \text{ au}$		
T_p versus V	0.372 ± 0.004	1.38 ± 0.01
$T_{ }$ versus V	0.419 ± 0.005	2.29 ± 0.02
T_{\perp} versus V	0.354 ± 0.005	1.15 ± 0.01

wind speed at 1 au (Wang & Sheeley 1990; Arge & Pizzo 2000) as

$$V(f_s) = 267.5 \text{ km s}^{-1} + \frac{410 \text{ km s}^{-1}}{f_s^{2/5}}. \quad (1)$$

In fact, an overexpansion of the flux tube, generally observed at the edge of the coronal hole, gives a slower stream with respect to the flux tube generated in the centre of the source, in agreement with simple acceleration models involving Alfvén waves (Wang & Sheeley 1991). Recently, Pinto, Brun & Rouillard (2016) have argued that some other ingredients are also needed to produce the large speed variability observed in the solar wind. However, the expansion factor seems to be sufficient within fast streams. Therefore, an expansion factor in the range [0.5, 3] can produce, within the same source, the variability in the bulk speed observed in our data sets, i.e. $V \in [530, 800] \text{ km s}^{-1}$.

The magnetic expansion factor is intrinsically related to the perpendicular component of the temperature. By using the first adiabatic invariant and assuming a double-adiabatic expansion of the plasma, we find

$$T_{\perp}(R) = T_{\perp}(R_{\odot}) \frac{1}{f_s} \left(\frac{R_{\odot}}{R} \right)^2, \quad (2)$$

with $T_{\perp} \sim 10^6 \text{ K}$ at $R \sim R_{\odot}$ (Dolei, Spadaro & Ventura 2016). A positive correlation between the perpendicular temperature and the bulk speed is already present in this simple equation. However, the slope is steeper than the one predicted at $35 R_{\odot}$ (see Fig. 4) and also the values of the temperature are much lower than expected (Perrone et al. 2019). Therefore, we could suppose that other physical processes, acting eventually when the wind is sub-Alfvénic, should

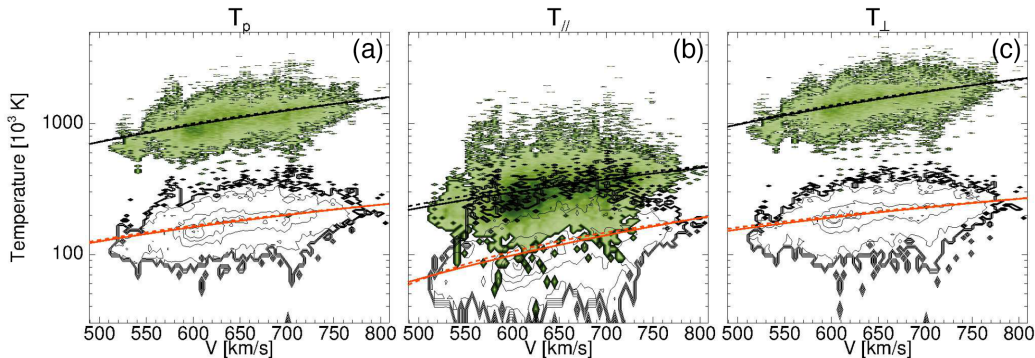


Figure 4. Colour-filled contour plots: expected T – V relationship in fast solar wind at $\sim 35 R_{\odot}$. Contour lines: corresponding T – V relationship at 1 au. Lines refer to the fits $T \propto mV$ (dashed) and $T \propto V^{\gamma}$ (solid) for $35 R_{\odot}$ (black filled) and 1 au (red open).

be taken into account to flatten the distribution and move it towards larger values of the temperature.

Moreover, the solar wind is not expanding adiabatically (Marsch et al. 1982; Hellinger et al. 2011; Perrone et al. 2019), so an external term of heating is needed to locally play a role during the wind expansion. Assuming a constant solar-wind proton speed, which is a valid approximation far from the Alfvénic point, the perpendicular heating rate, independent of speed and produced by physical processes that depend on the expansion time rather than radial distance, can be written as (Hellinger et al. 2011)

$$Q_{\perp}(R) = nk_B (\mathbf{V} \cdot \nabla T_{\perp} + T_{\perp} \nabla_{\perp} \cdot \mathbf{V}), \quad (3)$$

where the radial evolution of the proton density is compatible with a constant radial velocity and $\nabla_{\perp} = \nabla - \nabla_{\parallel}$ with $\nabla_{\parallel} = \mathbf{b}(\mathbf{b} \cdot \nabla)$, \mathbf{b} being the unit vector along the magnetic field. Therefore, the perpendicular temperature related to external heating, i.e. derived from equation (3) and where both the radial dependences of Q_{\perp} ($\propto R^{-4}$; Hellinger et al. 2011) and density ($n \propto R^{-2}$; Perrone et al. 2019) are taken into account, can be written as

$$T_{\perp}(R) = q_{\perp} \frac{1}{V} \frac{R_{\odot}}{R}, \quad (4)$$

with all the constants of the derivation included in

$$q_{\perp} = \frac{Q_{\perp}(R_E) R_E^2}{k_B n(R_E) R_{\odot}} \sim 10^{10} \text{ K km s}^{-1}, \quad (5)$$

where $R_E = 1 \text{ au}$ and $Q_{\perp}(R_E) \sim 2 \times 10^{-17} \text{ W m}^{-3}$ (Hellinger et al. 2011). Here, the temperature is anticorrelated with the speed, meaning that the mechanisms of heating are more efficient in slower streams, in agreement with the results in Section 2.2.

The qualitative radial evolution of the T – V relationship, for the perpendicular component of the temperature, could be reasonably well reproduced by a simple model where tube geometry and heating, which have different relative importance at different radial distances, are the very basic ingredients. On one hand the expansion factor of a tube can naturally produce a T – V correlation within the same stream. On the other hand, assuming a constant heating rate with respect to the speed, the different transit time alone can roughly produce the change in the slope that is found in the observations. Moreover, since the main contribution to the total temperature is given by T_{\perp} , consistent with this being typical fast wind (Stansby, Matteini & Horbury 2019), the radial evolution of the T – V relationship for T_{\perp} is observed to be similar to that of T_p . Therefore, we could suppose that our model is able to roughly explain also the observations for the total temperature. Conversely, since the radial behaviour of the parallel counterpart is not so clear, it is very difficult to model it taking into account only simple processes. Note that the expansion model, leading to equation (2), does not produce an equivalent T – V relation for T_{\parallel} . It is worth noting that the proposed model is very simplified and many assumptions are in place. First of all, the external heating is more complex and it is very possible that it actually depends on speed. Several mechanisms, related to the propagation (parallel to the magnetic field) and/or diffusion (perpendicular to the magnetic field) of protons, have been proposed for the ion heating in the solar wind that could reduce the temperature gradient. Among them, the ion-cyclotron resonance can produce heating (Hollweg & Markovskii 2002). Moreover, a quasi-linear diffusion of the proton core can be risen by the ion-cyclotron kinetic Alfvén waves that can locally be excited at the expense of the free energy contained in the double beam ion distributions (Voitenko, Goossens & Marsch 2001). An alternative model is non-resonant stochastic heating (Chandran et al.

2010), based on the violation of magnetic moment conservation. Furthermore, it has been also shown that the interaction of particles with coherent structures, related to flux tube boundaries (Greco et al. 2008) and intermittent structures generated by turbulence (Perrone et al. 2017), can locally produce an enhancement of heating (Osman et al. 2011, 2012; Wu et al. 2013). Finally, the external heating could also depend on the different amount of intermittent enhancements in plasma speed, namely spikes (Horbury et al. 2018), observed in fast streams. Their contribution could be more important in the regions close to the Sun, since as the plasma moves away from the Sun, the amplitude of the spikes decreases, constrained by the Alfvén speed (Matteini et al. 2014, 2015; Perrone et al. 2019).

4 SUMMARY AND CONCLUSIONS

It is well known that a strong correlation exists between temperature and flow speed of the solar wind. Here, we quantitatively study the T – V relationship in a well-defined stream of coronal-hole plasma (Perrone et al. 2019), by means of reprocessed proton-core data from both the *Helios* probes.

We show for the first time that the temperature–speed relationship evolves within the same stream as the solar wind radially expands in the inner heliosphere, meaning that it is misleading to use the T – V relationship at 1 au as a proxy for that near the Sun. In particular, we observe that the T – V relationship for T_{\perp} (and correspondingly T_p) becomes flatter as the plasma approaches the Earth. On the other hand, we find no clear dependence for T_{\parallel} , whose speed distribution, always lower than the one for T_{\perp} , contributes less to the distribution of the total temperature. This implies that an increase in speed produces a preferential increase of the perpendicular temperature.

We suggest a very simple model that combines basic ingredients (i.e. tube geometry and heating depending on the transit time) to describe the radial behaviour of the T – V relationship for T_{\perp} . In particular, the expansion factor of a tube can produce a positive T – V correlation within a single stream, while the different transit time can lead to a flattening of the slope. However, this is a zero-order approximation and a more complex and self-consistent description is needed to explain the observations, which is beyond the scope of this work.

We also find, by means of the individual T – V relationship at different heliocentric distances, that the cooling index of the radial evolution of the proton temperature depends on the speed. In fact, the radial cooling of T_{\perp} becomes steeper in faster streams, suggesting that they have less time to interact with the mechanisms responsible of the perpendicular heating. On the other hand, for the cooling of T_{\parallel} we observe an opposite behaviour. A first dependence of the cooling index on the flow speed, which monotonically increases with decreasing velocity, has been observed by Eyni & Steinitz (1981). However, strong systematic effects have characterized their analysis. In fact, they used the radial component of the temperature that gives a different measure of the total temperature fraction at different heliocentric distance, enhancing the dependence of the cooling rate on flow velocity. Moreover, they used published data from different missions, namely *Mariner 2*, *Helios 1*, and *Pioneer 10*, which were averaged over very different scales. Finally, their data set suffered from effects due to stream–stream interactions and averaging over large flow-velocity variance.

Finally, we predict the T – V relationship for fast solar wind at the distance of the first three perihelia of *Parker Solar Probe*, i.e. $\sim 35 R_{\odot}$. We extrapolate the values of the temperature within each interval listed in Table 1, by using the speed-dependent cooling indices. We expect that this extrapolation is reliable far from the

Alfvénic point. Below this region, the processes of acceleration of the solar wind could play a crucial role in determining the thermodynamics of the plasma, and *Parker Solar Probe* will help in this exploration. In the same way, we extrapolate the T - V relationship for fast wind at 1 au and we find a quite different correlation with respect to previous studies (Lopez & Freeman 1986; Elliott et al. 2012). The differences could be due to the fact that (i) we use a homogeneous data set with plasma coming from the same coronal hole, while Lopez & Freeman (1986) and Elliott et al. (2012) used an extensive data set, mixing several sources and containing also regions of interaction between slow and fast wind; (ii) we consider the proton-core temperature, instead of the second-order moment of the proton distribution function where the presence of secondary beams cannot be removed; (iii) we analyse variations of the temperature on smaller scales (~ 40 s) with respect to the hourly averages of plasma parameters used in previous studies; and (iv) we use speed-dependent cooling indices to remove the effects of the radial distance.

ACKNOWLEDGEMENTS

Work by DP and TSH was supported by STFC grant ST/N000692/1; DS was supported by a studentship under STFC grant ST/N504336/1; and LM was supported by the Programme National PNST of CNRS/INSU co-funded by CNES.

REFERENCES

- Arge C. N., Pizzo V. J., 2000, *J. Geophys. Res.*, 105, 10465
- Borovsky J. E., Thomsen M. F., Elphic R. C., 1998, *J. Geophys. Res.*, 103, 17617
- Burlaga L., Ogilvie K. W., 1970, *ApJ*, 159, 659
- Chandran B. D. G., Li B., Rogers B. N., Quataert E., Germaschewski K., 2010, *ApJ*, 720, 503
- Démoulin P., 2009, *Sol. Phys.*, 257, 169
- Dolei S., Spadaro D., Ventura R., 2016, *A&A*, 592, A137
- Elliott H. A., Henney C. J., McComas D. J., Smith C. W., Vasquez B. J., 2012, *J. Geophys. Res.*, 117, A09102
- Eyni M., Steinitz R., 1981, *ApJ*, 243, 279
- Fox N. J. et al., 2016, *Space Sci. Rev.*, 204, 7
- Greco A., Chuychai P., Matthaeus W. H., Servidio S., Dmitruk P., 2008, *Geophys. Res. Lett.*, 35, L19111
- Hellinger P., Matteini L., Stverák S., Trávníček P. M., Marsch E., 2011, *J. Geophys. Res.*, 116, A09105
- Hellinger P., Trávníček P. M., Stverák S., Matteini L., Velli M., 2013, *J. Geophys. Res.*, 118, 1351
- Hollweg J. V., Markovskii S. A., 2002, *J. Geophys. Res.*, 107, 1080
- Horbury T. S., Matteini L., Stansby D., 2018, *MNRAS*, 478, 1980
- Lopez R. E., Freeman J. W., 1986, *J. Geophys. Res.*, 91, 1701
- Marsch E., Muhlhauser K.-H., Schwenn R., Rosenbauer H., Pilipp W., Neubauer F. M., 1982, *J. Geophys. Res.*, 87, 52
- Matteini L., Horbury T. S., Neugebauer M., Goldstein B. E., 2014, *Geophys. Res. Lett.*, 41, 259
- Matteini L., Horbury T. S., Pantellini F., Velli M., Schwartz S. J., 2015, *ApJ*, 802, 11
- Matthaeus W. H., Elliott H.-A., McComas D. J., 2006, *J. Geophys. Res.*, 111, A10103
- Muller D., Marsden R. G., St. Cyr O. C., Gilbert H. R., 2013, *Sol. Phys.*, 285, 25
- Neugebauer M., Snyder C. W., 1966, *J. Geophys. Res.*, 71, 4469
- Osman K. T., Matthaeus W. H., Greco A., Servidio S., 2011, *ApJ*, 727, L11
- Osman K. T., Matthaeus W. H., Hnat B., Chapman S. C., 2012, *Phys. Rev. Lett.*, 108, 261103
- Perrone D., Alexandrova O., Roberts O. W., Lion S., Lacombe C., Walsh A., Maksimovic M., Zouganelis I., 2017, *ApJ*, 849, 49
- Perrone D., Stansby D., Horbury T. S., Matteini L., 2019, *MNRAS*, 483, 3730
- Pinto R. F., Brun A. S., Rouillard A. P., 2016, *A&A*, 592, A65
- Richardson J. G., Cane H. V., 1995, *J. Geophys. Res.*, 100, 23397
- Schwadron N. A., McComas D. J., 2008, *ApJ*, 686, L33
- Stansby D., 2017, Helios Proton Core Parameter Dataset. Available at: <http://doi.org/10.5281/zenodo.1009506>
- Stansby D., Salem C., Matteini L., Horbury T., 2018, *Sol. Phys.*, 293, 155
- Stansby D., Matteini L., Horbury T., 2019, *MNRAS*, 482, 1706
- Strong I. B., Asbridge J. R., Bame S. J., Heckman H. H., Hundhausen A. J., 1966, *Phys. Rev. Lett.*, 16, 631
- Voitenko Yu., Goossens M., Marsch E., 2001, in Battrock B., Sawaya-Lacoste H., eds, Proceedings of the First Solar Orbiter Workshop: Solar Encounter. ESA SP-493, ESA, Noordwijk, p. 411
- Wang Y.-M., Sheeley N. R., Jr, 1990, *ApJ*, 355, 726
- Wang Y.-M., Sheeley N. R., Jr, 1991, *ApJ*, 372, L45
- Wu P. et al., 2013, *ApJ*, 763, L30

This paper has been typeset from a $\text{\TeX}/\text{\LaTeX}$ file prepared by the author.